White Paper

Agilent
Trusted Answers

Investigating the Use of the Agilent 8700 LDIR Chemical Imaging System in Published Literature

Author

Yasurika Heenatigala
Agilent Technologies, Inc.

Abstract

The Agilent 8700 Laser Direct Infrared (LDIR) chemical imaging system, combined with Agilent Clarity software, has been demonstrated by leading research groups worldwide as a versatile platform for rapid, automated, and spatially resolved chemical analysis. The system's ability to deliver high-quality imaging and spectral data quickly expands research and industrial capabilities in quality control, authenticity verification, and advanced material innovation.

This white paper provides a comprehensive summary of how active researchers around the world are utilizing the 8700 LDIR in their diverse scientific applications.

Introduction

Laser direct infrared (LDIR) spectroscopy has quickly proven itself as an efficient analytical technique for quick identification and characterization of samples through chemical imaging and infrared (IR) spectral analysis. LDIR imaging integrates microscopic (spatial) and mid-infrared (mid-IR) vibrational spectroscopic methods to create high-resolution visual maps of a sample's chemical composition, structure, and molecular dynamics.[1]

The Agilent 8700 LDIR chemical imaging system combines the molecular specificity of mid-IR spectroscopy, with the speed of a quantum cascade laser (QCL) and rapidly scanning optics, to provide actionable high-quality imaging and spectral data in minutes. This instrument has helped researchers make groundbreaking progress in microplastics research and monitoring studies.

In this white paper, we provide a comprehensive summary of how active research groups around the world are utilizing the Agilent 8700 LDIR chemical imaging system in other diverse scientific and industrial applications, spanning food and beverage, advanced biomaterials, pharmaceutical formulations, and geoscience. The applications mentioned are summarized as follows.

Advanced biomaterials[2]

A study conducted by Alvarez-Fernandez and a multi-institutional team from the Materials Physics Center and IKERBASQUE-Basque Foundation for Science (Spain), and the University of Cambridge Institute for Medical Research (England), explored the fabrication of spiral-like peptide nanostructures, using short self-assembling peptides derived from the SARS-CoV-2 Spike fusion domain. The 8700 LDIR system was employed in reflection mode to analyze the amide I band for confirming peptide secondary structures within the nanostructure fibrils. The LDIR spectra explained crucial morphological distinctions in the fibrils, such as revealing fibrils with flexible morphology predominantly adopted antiparallel β-sheet conformations, developing understanding for optical and nanofabrication applications.

Geoscience[3,4]

Gordon and researchers, from Michigan-based Lake Superior State University (U.S.), assessed the 8700 LDIR system for rapid, nondestructive characterization of rocks and minerals using polished geological hand samples. The LDIR generated hyperspectral and multispectral datasets, spectral matched against the U.S. Geological Survey version 7 spectral library. The LDIR images rapidly distinguished mineral phases and grain morphology, demonstrating high capacity in the 8700 LDIR as an identification tool.

Quantification in cellular agriculture[5]

Zhou and a collaborative research group, from Qingdao-based Ocean University of China, Qingdao Institute of Marine Bioresources for Nutrition and Health Innovation, and Qingdao National Library for Marine Science and Technology (China), investigated the scalable production of large-pore-sized edible porous microcarriers (EPM), for EPM-based food structuring techniques, in facilitating industrial-scale production of cultured fish meat. The LDIR was employed for precise particle counts in specified unit mass of EPM powder samples, supporting consistent cell seeding densities in upstream cell culturing processes.

Pharma: Evaluating distributional homogeneity[6]

A study conducted by Sacre and researchers, from the University of Liege (Belgium), evaluated the 8700 LDIR system for assessing distributional homogeneity of active pharmaceutical ingredients (APIs) and excipients in tablet formulations. The 8700 LDIR imaging was comparable with images of confocal Raman mapping, but at significantly reduced analysis times (7.5 minutes versus 4 hours), demonstrating promising potential for routine quality control and formulation development.

Pharma: Comparing LDIR against other established spectroscopic chemical imaging techniques[7]

An academic-industry collaboration between Carruthers *et al*., from the University of Strathclyde (Glasgow), and Clark and Clarke, from Pfizer Ltd., Sandwich (U.K.), evaluated LDIR chemical imaging for pharmaceutical formulations, particularly for characterizing spatial distribution of components, compared against Raman, near-infrared (NIR), and scanning electron microscopy-energy dispersive X-ray spectroscopy (SEM-EDX). The LDIR provided effective and rapid characterization of differences in size and spatial distribution of components, highlighting compelling capability for supporting manufacturing process understanding and troubleshooting.

Pharma: Capturing physiochemical properties[8,9]

Zaker and colleagues, from the Center for Drug Evaluation and Research division of the U.S. FDA, developed LDIR classification imaging methods to capture critical physicochemical properties of in-house prepared and over-the-counter tablets, focusing on the optimization of wavenumber selection and pixel size for rapid data acquisition. The 8700 LDIR showed effective agreement with Raman imaging, detecting a greater number of API domains with a smaller mean Feret diameter, but at reduced acquisition times by approximately 100 fold.

Tissue analysis[10]

Ojha and team, from the Indian Institute of Technology Kharagpur and the Institute of Reproductive Medicine, Kolkata (India), fabricated a multilayered biodegradable cervical stent to provide a treatment alternative for cervical reconstruction in patients with cervical atresia. The 8700 LDIR system was used for localization studies of extracellular matrix (ECM) proteins and tissue integration studies of explants, providing in situ molecular and structural insights without sample processing or labeling.

For Research Use Only. Not for use in diagnostic procedures.

Food and beverage[11]

Da Costa Filho and research group, from Nestlé Research (Switzerland), investigated the 8700 LDIR system for rapid detection, identification, and semi-quantification of adulterants in food ingredients. The 8700 LDIR system screened various adulterated food matrices within minutes, demonstrating significant sensitivity. Challenges were discussed, such as the difficulty of detecting adulterants that are homogeneously dispersed in wet-blended samples. Overall, the system illustrated capacity for economically motivated adulteration screening.

8700 LDIR chemical imaging system

Traditional vibrational spectroscopic techniques have established a significant foundation across various applications; however, challenges in analysis serve notable pain points to users[12], such as lengthy data acquisition times required to obtain high-definition chemical images of a sample surface[7], alongside limitations in resolution, tunability, and consequent extensive data processing.[8,9] Typically, these techniques involve the collection of a full spectrum at every point, significantly increasing imaging data collection times and limiting their practicality for large-scale analysis. To address this, new technologies have begun incorporating chemical imaging systems coupled with a high-intensity, broadly tunable QCL, accelerating a fundamentally different approach to chemical imaging. With QCL technology, it is possible to focus on distinct spectral bands to obtain distribution maps of a targeted component, decreasing imaging time by an order of magnitude and offering new opportunities for practical and real-time characterization of materials.

The Agilent 8700 LDIR chemical imaging system is equipped with a proprietary QCL light source, a thermometrically cooled single-point mercury-cadmium-telluride (MCT) detector, and rapid-scanning optics to enable speed in reflection-based IR imaging. The instrument is equipped with a total of four imaging modes: two visible—wide field of view and high magnification—and two IR—direct reflectance, attenuated total reflectance (ATR)—. The system covers the spectral range of 1800 to 975 cm−1, housing the mid-IR fingerprint region, which contains unique patterns of absorption bands used to differentiate between molecules and are crucial in confirming compound identity.

The 8700 LDIR is complemented by Agilent Clarity software, facilitating load-and-go workflows, data interrogation, and reporting. Delivered in an intuitive visual interface, Clarity software enables fast and easy method creation, automated workflows, spectral analysis using mathematical functions and spectrum transformations, and user-generated spectral libraries for component matching with hit quality indices. The 8700 LDIR provides two dedicated modes of workflows for particle analysis. In the first mode, Scan, the IR frequency is parked (that is, a single wavelength is selected) while the optics move at high speed over the sample, reflecting the light back into the detector. In the second mode, Sweep, the optics are parked at a single point over the sample while the QCL sweeps through the frequency range, obtaining a full spectrum. In conjunction, Scan may be used to locate particles of interest in a sample, and Sweep can be used for spectral identification.

Agilent LDIR accessories and supplies enable easy sample preparation. The right tools for the task ensure you can analyze and characterize your sample rapidly and accurately. Table 1 outlines the intended use and application of several Agilent accessories and supplies for use with the 8700 LDIR.

The 8700 LDIR has been widely adopted in microplastics research, where its ability to automatically detect, identify, and quantify particles across large sample areas has provided valuable advances in environmental monitoring. However, the unique strengths of the system, including robust imaging speeds, high spatial resolution, load-and-go workflows, and user-customizable methods, make it suitable for a much broader range of scientific and industrial applications.

Table 1. Agilent accessories and supplies for use with the Agilent 8700 LDIR.

Application	Accessories and Supplies	Intended Use
Multilayer Analysis	**LDIR sample planar** No power supply, maintenance free	Planing a flat, uniform sample surface. Controls micron-scale thickness with simple manual adjustment. The 8700 LDIR system's quantitative performance depends on consistent interaction depth with the IR beam.
	Microtome blade, diamond-finish 50/pk	Sectioning thin, smooth cross-sections. Ceramic-coated, diamond-finish blades providing mechanical strength and cutting precision. Suitable for cutting polymers, coatings, and adhesives.
	Sacrificial laminate strip 128/pk	Supporting controlled planing, sectioning, and preparation of multilayer laminates without direct damage to the region of interest.
	Adhesive UV-cured, low-shrink, 10 mL syringe	Glueing with low outgassing and low coefficient of thermal expansion, preserving chemical integrity for analysis. Bonds metals, ceramics, glass, and plastics.
	Glue dispensing tips Tapered 18 GA, 150/pk	Dispensing tip for glue. Provides controlled, smoothed flow.
Solid Samples Analysis	**Glass microscope slide** – 25 × 25 mm, 200/pk – 75 × 25 mm, 100/pk	Mounting samples. Provides mechanical flatness and ease of mounting. Suboptimal due to IR transmission losses in reflection geometry.
	Low-e (Kevley) slide 25/pk	Low-emissivity slides are highly reflective of IR light, reducing background spectral noise while maximizing signal return.
	Slide sample holder kit 1 slide holder	For use with (holds) low-e (Kevley) slides.
Liquid Samples Analysis	**Gold-coated filter** 25 mm diameter, 0.8 µm pore size, 25/pk	Consists of a polyester membrane (PET) with a gold layer of 100/0 nm. Provides chemically inert and uniform reflectance, and minimal spectral contribution, for high-precision studies.
	Aluminium-coated filter 25 mm diameter, 0.8 µm pore size, 25/pk	Consists of a PET membrane with an aluminum layer of 100/0 nm. Reliable and cost-effective alternative for high-throughput studies.[13]
	25 mm filter holder kit 1 (two-position) holder	Two-position sample holder kit for 25 mm diameter filters.

Figure 1. The Agilent 8700 LDIR chemical imaging system, with the Agilent Clarity software shown on the monitor analyzing a sample.

Research applications of the 8700 LDIR chemical imaging system

Research groups located around the world have used the 8700 LDIR in diverse applications. A review of published approaches in the last six years is presented in this section.

Advanced biomaterials

Peptide-Guided Self-Assembly: Fabrication of Tailored Spiral-Like Nanostructures for Precise Inorganic Templating[2]

Alvarez-Fernandez and their comprised team, from the Materials Physics Center and IKERBASQUE-Basque Foundation for Science (Spain), and (the University of) Cambridge Institute for Medical Research (England) pursued short self-assembling peptides (SAPs), derived from the SARS-CoV-2 Spike fusion domain, as building blocks to form spiral-like nanostructures at air-water interfaces. These nanostructures were used as templates for the fabrication of metallic replicas, of which the authors were interested in investigating the unique optical, electronic, and catalytic properties associated with the chirality and metallic species of the respective spiral. The aim of the study was to expand potential applications in optical and nanofabrication technologies.

Building on previous similar research conducted by Huang *et al.*[14,15], Zhang *et al.*[16], and Wen *et al.*[17], Alvarez-Fernandez and coresearchers identified persisting challenges limiting the practical applications of the fabrication methodologies used to produce nano-spiral structures. Such challenges included the need for the incorporation of functional groups that promote self-assembly, the limited structural control over the resulting nanostructures, and difficulties in applying the methodologies to metallic structures. Therefore, the team investigated SAPs as an alternative material capable of producing tailored and precisely controlled nanostructures. They also pursued the use of interfacial assembly—a promising fabrication technique capable of forming and tuning the complex spiral nanostructures by providing a conducive platform for the spontaneous self-assembly of colloidal systems, driven by a reduction in interfacial energy.

Two Spike fusion peptides were used in the study for the nanostructure templates: FP1 (SARS-CoV-2 816–837) and FP2 (835–856), which are characterized by their short length and hydrophobicity. The authors found that at an air/water interface, a uniaxial (lateral) compression (using a Langmuir-Blodgett trough) imposed an interfacial flow, allowing the tuning of the morphology, orientation, and packing density of the self-organized nanostructures formed by the peptides. Notably, the authors found, through atomic force microscopy (AFM) analysis, that at a controlled compression speed of 0 mN m^{-1}, peptide aggregates were random, as shown in Figures 2B (FP1) and C (FP2). They also found that an increase to speed of 20 mN m^{-1} promoted the formation of elongated and flexible nanofibrils (for both FP1 and FP2) consisting predominantly of β-strands sheet structure, as shown in Figures 2D (FP1) and E (FP2).

The 8700 LDIR was employed to confirm the presence of peptide secondary structures within the self-assembling observed fibrils. The authors measured the peptide fibrils on Au-coated filters, setting up the system in reflection mode focusing on the amide I band, around 1,600 to 1,700 cm^{-1}. The amide I band is widely recognized for its sensitivity to protein secondary structure, associated with the stretching vibration of the carbonyl group. To minimize potential interferences from water band absorption (around 1,630 to 1,650 cm^{-1}), the researchers stored the samples under vacuum for 48 hours prior to measurement.

The LDIR spectra of FP1 and FP2 sample surfaces are shown in Figure 2H. In Figure 2I, their amide I bands are shown deconvoluted into the prominent absorption bands with corresponding secondary structures.
Alvarez-Fernandez and team found that FP2 spirals showed strong absorption around 1,623 cm^{-1}, indicative of peptides adopting β-sheet confirmations. Interestingly, the authors observed strong perpendicular mode at ~ 1,620 cm^{-1} and weaker intensity parallel mode at 1,680 cm^{-1}, consistent with antiparallel β-sheets. In comparison, FP1 exhibited a broader mix of β-sheets, α-helices, and random coils (strong absorption band in region 1,620 to 1,650 cm^{-1}). These conformational distinctions provided a molecular explanation for the differences in morphology between the two peptides—that is, why FP2 formed flexible fibrils with spiral morphologies while FP1 assembled into stiffer, rod-like, straight fibrils.

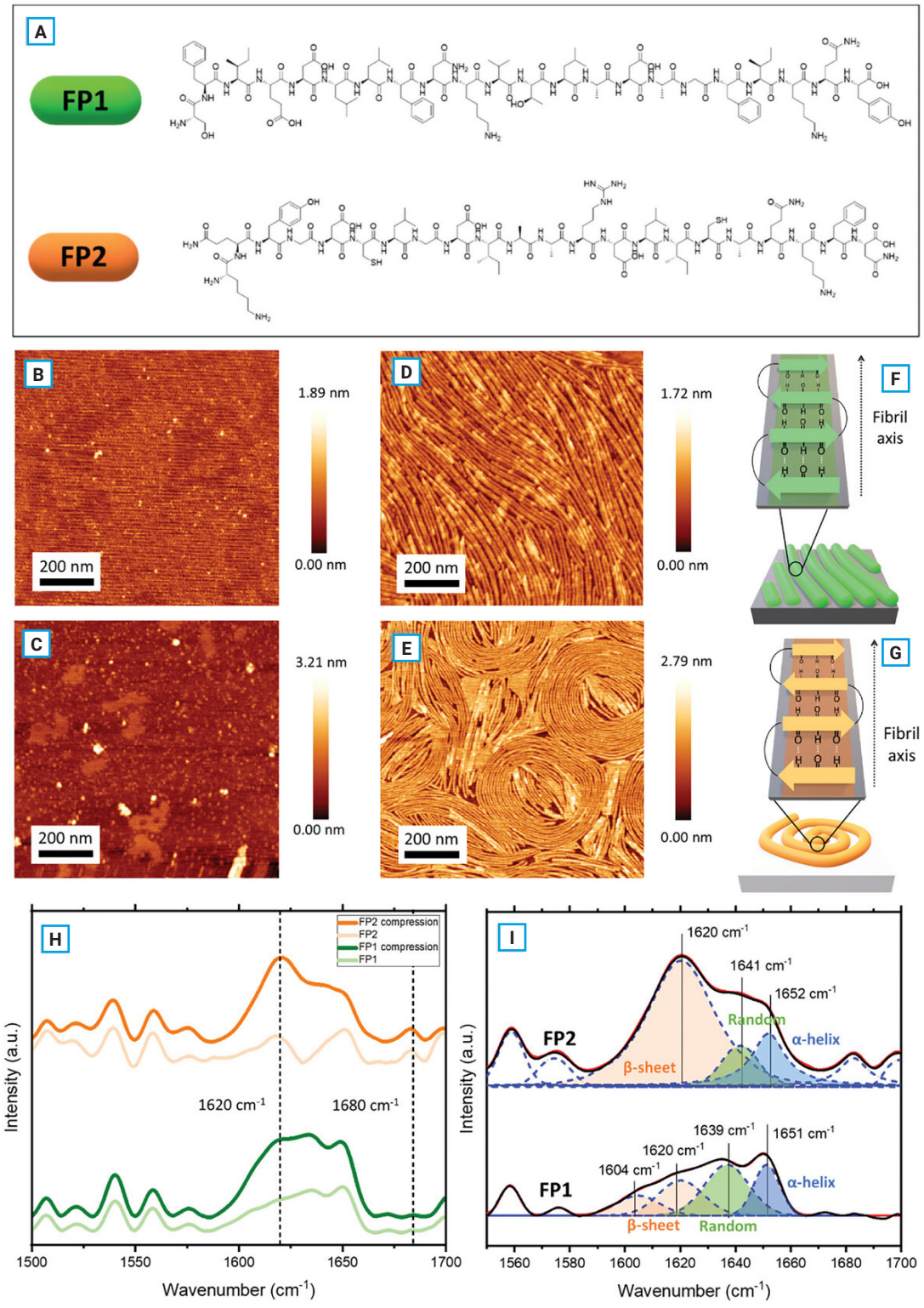

Figure 2. (A) Chemical structure of FP1 and FP2 peptides. (B–E) AFM micrographs of FP1 at (B) no compression and at (D) 20 mN m^{-1}, and of FP2 at (C) no compression and (E) at 20 mN m^{-1}. (F–G) Schematic representation of the β-sheets secondary structure, leading to the formation of the fibers. (H) LDIR spectra of samples. (I) Deconvolution of amide I band into prominent absorption regions. Reprinted with permission from Alvarez-Fernandez et al., *Adv. Funct. Mater.* **2024**, *35(1)*, 2411061. Copyright © 2024 The Authors. Advanced Functional Materials published by Wiley-VCH GmbH.

Geoscience

LDIR Spectroscopy Hyperspectral Imaging: Applications in Geochemical Phase Mapping and Interpretation of Multidimensional Analysis[3,4]

Gordon and researchers, from Lake Superior State University, based in Michigan U.S., assessed the 8700 LDIR as a nondestructive and rapid screening tool for the characterization of rocks and minerals, citing that common techniques in the minerology and geochemistry fields (such as powder X-ray diffraction and petrographic microscopy) are destructive and labor intensive.

The researchers performed chemical imaging on a variety of geological hand samples (up to 27 × 72 mm), creating hyperspectral and multispectral datasets, with the aim to produce a framework by which other analysts can utilize QCL instruments in novel ways.

Samples were polished flat and mounted on a standard microscope slide for hyperspectral analysis and imaging, with the authors citing that a benefit to using this technology in this application is that "while samples require smooth and parallel faces, they don't need to be brought to thin section."

The online U.S. Geological Survey (USGS) spectral library (version 7) includes spectra collected in the IR region by reflectance of ~ 90 common minerals. Using the USGS spectral library, a library for spectral matching was generated on the Clarity software. For data collection methods, the researchers set 10 µm pixel size, and 4 cm^{-1} spectral resolution. Then, data was exported as HDR images for processing by internally produced, publicly available Python scripts (https://github.com/ngordon0110/LDIR_HPS). The team created two main scripts: one matches collected spectra with the library through cosine similarity, and the other finds similarities between collected spectra through principal component analysis (PCA).

For each collected spectra, the team compared each pixel to the library, generating a cosine similarity score from 0 to 1. Figure 3 exhibits a produced cosine similarity map for calcite (A) and wollastonite (B) comparing the sample spectra to the USGS database. In addition, Figure 4 exhibits variance between collected spectra features, which the authors found had potential as an independent technique to identify regions of interest for further analysis, without the need for spectral library matching.

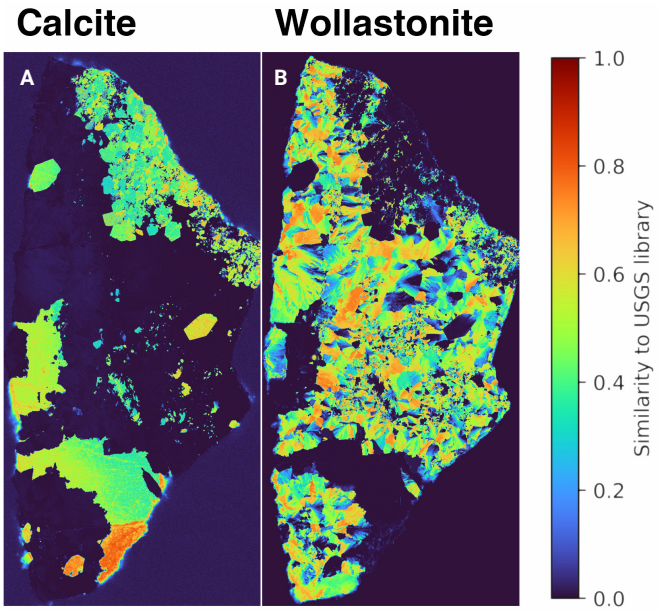

Figure 3. Cosine similarity maps comparing collected spectra to USGS database.

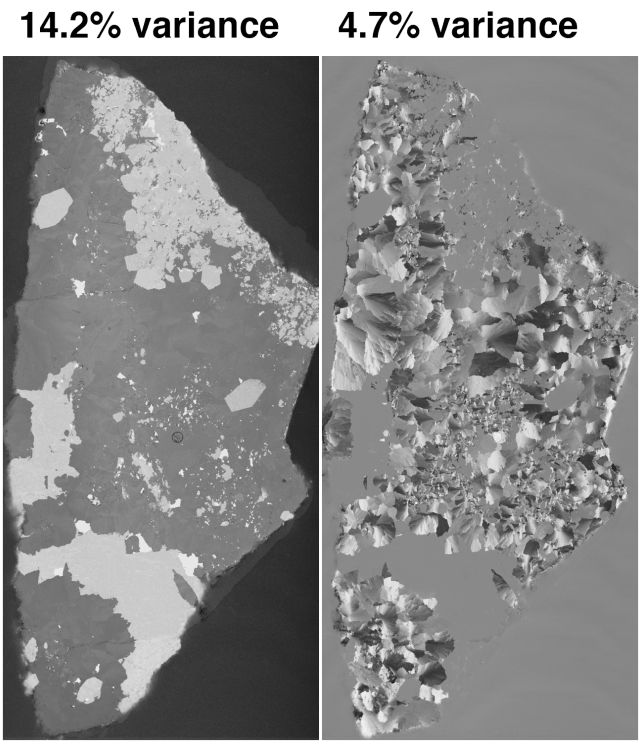

Figure 4. LDIR hyperspectral principal component analysis with explained variance. Reprinted with permission from Gordon *et al.*, Earth and Space Science Open Archive. Copyright © 2024 The Authors. Distributed via ESS Open Archive.

Gordon and team were interested in utilizing the 8700 LDIR as a complementary tool to traditional methods of identification to expedite and simplify the process. In the LDIR hyperspectral images, the authors observed distribution of minerals (heat maps) that revealed grain boundaries, differences in crystal structures, and crystal twinning in hand samples. Their results demonstrated promising potential for mineral phase mapping, grain mapping, and grain morphology, with limited sample preparation compared to traditional techniques.

Key quote from the study:

"Results suggest that LDIR may be helpful with rapidly distinguishing mineral phases and grain morphology on polished samples up to 27 × 72 mm."

Quantification in cellular agriculture

Scalable Production of Muscle and Adipose Cell-Laden Microtissues Using Edible Macroporous Microcarriers for 3D Printing of Cultured Fish Fillets[5]

A study conducted by the combined efforts of Zhou *et al.*, from Qingdao-based Ocean University of China, Qingdao Institute of Marine Bioresources for Nutrition & Health Innovation, and Qingdao National Library for Marine Science and Technology, China, investigated the production of large-pore-sized edible (macro)porous microcarriers (EPMs) for EPM-based cell expansion and food structuring techniques, to support industrial (large-scale) production of cultured fish meat.

Zhou and team noted the increasing need for high-quality protein amidst growing global population demands, with cultured meats gaining traction as a sustainable and eco-friendly meat alternative. They realized that research on cell-cultured meats is still in its infancy, largely due to challenges in scaling from laboratory to production. Culture growth can be limited by seed cell line, culture media, cell expansion techniques, and cell-to-meat conversion techniques. For example, the authors cited that seed cells from animal biopsies are typically adherent-dependent cells, and therefore their growth is by adherent-dependent proliferation limiting self-expansion capabilities.

To address this issue, the team identified a scalable approach involving the use of high-surface-area microcarrier suspension culture platforms, with current applications in the medical field. These platforms serve as temporary scaffolds during cell harvesting, allowing the required cellular adhesion, growth, and diffusion to support culture expansion to large scale. Noting that most commercially available microcarriers typically lack food-grade standardization or contain toxic substances introduced by manufacturing processes, the team developed EPMs and methods for introducing microporous structures within the EPMs that are safe for agricultural and food production purposes, enabling the EPMs to become building blocks in the assembly of meat analogs.

Zhou and team used muscle satellite cells (SCs) and adipose-derived stem cells (ASCs) from large yellow croakers, as well as fish gelatine and microbial transglutaminase in a precursor cross-linking agent solution for the microcarrier scaffold. The researchers found that enriching the precursor solution with NaCl during a freezing process could influence EPM pore size. Greater NaCl concentration reduced availability of cross-linkable groups in gelatine and increased free water available for crystallization. This led to larger-pore formation in the EPMs, which offered greater space and flexibility for cell growth and reshaping. After sterilization, the authors stated that the EPMs presented as white powder.

The team employed the 8700 LDIR to quantify the number of microcarrier particles in EPM powder samples of varying NaCl concentration. Each sample weighed 3 mg. Averaging particle density across the samples, the researchers quantified ~ 2,000 microcarriers per mg. The quantification was beneficial in finding that 600 g fish gelatine can yield 485.21 g EPMs, and in ensuring consistent cell seeding densities that could otherwise affect tissue formation.

As per Zhou *et al.*, scaffold optimization is crucial for cell loading in cultured meat, to meet quality equivalence of native meat. Following consecutive expansions, SCs and ASCs densities reached a 499- and 461-fold increase in cell numbers, respectively, enabling mature microtissue to be incorporated into a bioink and 3D printing of cultured fish fillets.

Pharma

Evaluation of Distributional Homogeneity of Pharmaceutical Formulation Using Laser Direct Infrared Imaging[6]

Sacre *et al.*, from the University of Liege, Belgium, evaluated the suitability of LDIR imaging for the analysis of pharmaceutical formulations—particularly, the distributional homogeneity of APIs and excipients within solid dosage forms. Distributional homogeneity of compounds in a pharmaceutical formulation is a key parameter to be monitored since it may affect the efficacy and safety of the formulation.

In this study, the model system was an in-house prepared tablet in a five-component formulation blend, with two APIs and three excipients—respectively, acetylsalicylic acid (20% w/w), paracetamol (20% w/w), lactose monohydrate (25% w/w), microcrystalline cellulose (30% w/w), and magnesium stearate (5% w/w). The tablets were analyzed using both Raman and LDIR imaging.

IR imaging methods were developed in Clarity software, with reference spectra for each pure compound acquired and stored in a spectral library. Univariate single peak ratio analyses (with baseline correction) were developed for each ingredient, then a multipeak method combined all compound-specific ratios to generate full-tablet distribution maps. Tablets (13 mm diameter) were scanned at 40 µm step size, covering the entire surface in ~ 2.5 minutes. As written by the authors, "once the method is developed, the analysis time is very short since it took 2.5 minutes between the start of the imaging experiment and the display of the results (31 seconds for each single peak analysis)." Data was then exported to MATLAB for distributional homogeneity index computation.

The tablets were sampled at seven different mixing time points, ranging from unmixed to fully blended. Each sample tablet was analyzed using both LDIR imaging and confocal Raman microscopy to compare the performance of the two imaging approaches, focusing on how each technique captures intratablet homogeneity and determines mixing end points during formulation development.

The researchers observed that both techniques successfully tracked the progressive improvement in homogeneity during mixing. However, the analysis times were different. While Raman imaging required a total analysis time of 4 hours per tablet to obtain the distribution map of acetylsalicylic acid with a step size of 100 µm, it took 7.5 minutes to achieve the same result with the 8700 LDIR. Overall, the team noted that LDIR achieved mostly similar results as Raman imaging in "30x less time." The authors highlighted this time-conserving benefit, stating "therefore, it is possible to analyze several tablets and get a unique insight into 'intratablet' homogeneity and 'intertablet' homogeneity. The latter is difficult to obtain with Raman imaging because of the long acquisition times making the analysis of several tablets difficult."

Key quotes from the study:

"The results obtained in the present study show that LDIR is a promising technique for the analysis of pharmaceutical formulations and that it could be a valuable tool when developing new pharmaceutical formulations."

"This might be very useful in routine analysis of pharmaceutical blends as quality control of the produced tablets, but most of all during the development of new formulations."

Evaluation of Laser Direct Infrared Imaging for Rapid Analysis of Pharmaceutical Tablets[7]

Carruthers, Faulds, and Graham from the University of Strathclyde, Glasgow, together with Clark and Clarke from Pfizer Ltd., Sandwich, UK investigated LDIR imaging as an important tool in the pharmaceutical industry for characterizing the spatial distribution of components within final drug products.

The study evaluated the capabilities of LDIR chemical imaging for pharmaceutical formulations and compared with other established spectroscopic chemical imaging techniques, such as Raman, NIR, and scanning electron microscopy-energy dispersive X-ray (SEM-EDX) spectroscopy. LDIR was evaluated as a novel technique that could overcome the limitations of current vibrational spectroscopic chemical imaging techniques, specifically in terms of data acquisition times and image resolution/quality. The authors demonstrated that LDIR imaging provided high-definition component distribution maps comparable to Raman and SEM-EDX at orders-of-magnitude faster in terms of time.

Referencing research conducted by Sacre *et al.*[6] (see previous paper), who evaluated LDIR imaging for assessing the homogeneity of components within a model pharmaceutical formulation and compared against confocal Raman mapping, the authors were interested in how the "study demonstrated that both techniques achieved comparable results, however the 8700 LDIR produced data with the same spatial resolution 32-fold faster." Carruthers *et al.* pointed out that the model system analyzed in Sacre and team's study contained two APIs at relatively high compositions (20% w/w each), resulting in relatively large component domains distributed across the tablet matrix. Therefore, they realized that the capabilities of the 8700 LDIR had not yet been explored for analyzing more complex systems containing lower concentrations of API that are more typical of real pharmaceutical formulations.

For that reason, Carruthers and team aimed to assess the capabilities of LDIR imaging in analyzing more complex formulations, and provided a comparison against the four other previously mentioned established spectroscopic imaging techniques.

In this study, the model system was an in-house prepared tablet in a three-component formulation blend containing an API—hydrobromide salt (5% w/w)—and two excipients—microcrystalline cellulose (MCC) (80% w/w) and saccharin (15% w/w)—all differing in their elemental composition. A commercially available pharmaceutical tablet containing the same API—80 mg of hydrobromide salt—was also examined to determine the capabilities of LDIR imaging for examination of real formulations. SEM-EDX was used to confirm the spatial arrangement of components.

Using Clarity software, the authors built a reference library of raw components. The reference library was built by (for each component) obtaining 10 spectra and averaging into a reference spectrum. Then, based on the reference spectra,

a single peak ratio analysis was developed with a unique peak/baseline position (wavenumber) automatically identified by Clarity software.

All LDIR data was collected with a spatial pixel size of 10 µm, and the same 3,000 × 3,000 µm sample area was imaged by all four techniques (Figure 5).

The authors found that the LDIR, Raman, and SEM-EDX chemical images revealed "very similar" domain size and shape of the excipient components. There was some variation in the number and size of API domains, with slight overestimation in the Raman data and underestimation in the LDIR data in comparison to the SEM-EDX data. However, the authors stated, "the resultant LDIR image does provide a comparable distribution of components and produces data at an order of magnitude faster than all other techniques." There was a notable difference in the quality of the image obtained by NIR, and in the size and distribution of components in the NIR image, compared with the other techniques.

Key quotes from the study:

"The LDIR chemical imaging approach provides the opportunity to obtain detailed domain morphology information in a fraction of the time, and would be ideal for routine analysis or as a rapid screening tool to characterize differences in the size and spatial arrangement of components for troubleshooting investigations."

"Comparison with other established spectroscopic chemical imaging techniques showed LDIR imaging provides high-definition component distribution maps comparable to Raman and SEM-EDX at orders of magnitude faster."

"The system could be a powerful tool for manufacturing process understanding…for formulations that have been processed under different manufacturing routes."

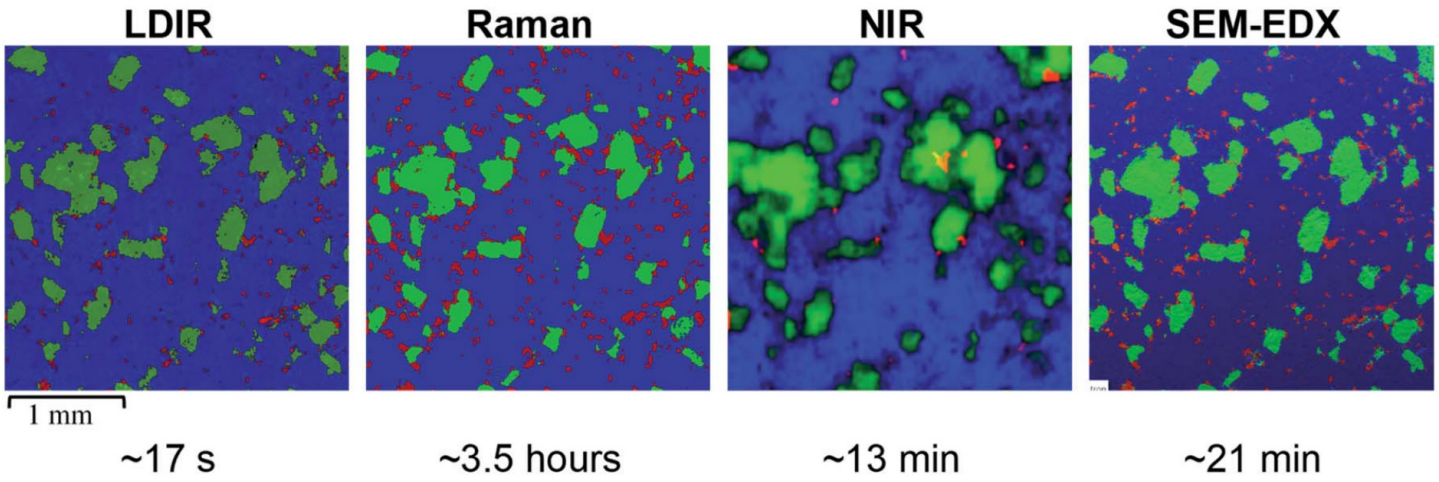

Figure 5. Chemical images of the three-component model system. Blue = microcrystalline cellulose, green = saccharin, and red = hydrobromide salt API. Each chemical image represents a 3,000 × 3,000 µm sample area. The total data collection time for each technique is displayed below the respective chemical image. Reprinted from Caruthers *et al.*, "Evaluation of laser direct infrared imaging for rapid analysis of pharmaceutical tablets" *Anal. Methods* **2022**, *14*, 1862–1871.

Advancing Pharmaceutical Tablet Analysis with LDIR Imaging[8,9]

Zaker and coworkers from the Center for Drug Evaluation and Research (CDER) division of the U.S. Food and Drug Administration (FDA) explored how LDIR imaging can be applied to pharmaceutical tablet analysis. The 8700 LDIR was used for hyperspectral imaging to capture critical physicochemical properties (such as chemical identity, particle size, shape, and distribution of components like APIs, excipients, and fillers). The authors developed a classification imaging method on Clarity software specifically for tablets, collecting reflectance images at select wavenumbers.

From previous research, the authors identified that the LDIR (specifically its QCL technology coupled with IR microscopy) could "overcome limitations in resolution, tunability, and data acquisition times found in conventional (Raman, IR, NIR) imaging"; however, the advantages came with the need for more extensive method development. The authors noticed a lack of generalized LDIR reflectance imaging approaches with classification methods for pharmaceutical applications, and therefore developed this study with the aim to produce an LDIR classification method through systematic analysis of a well-characterized, in-house prepared tablet. Therefore, Zaker and team investigated wavenumber selection for peak/baseline points and step (pixel) size as key aspects of LDIR imaging method development for pharmaceutical analysis. LDIR images were compared with Raman images to evaluate accuracy and resolution of the 8700 LDIR method.

The model system included two in-house tablet blend formulations with an API, midodrine hydrochloride (HCl), and two excipients—microcrystalline cellulose (MCC) and cornstarch (CS). Both tablet formulations contained 2% w/w API but differed in excipients, with tablet A containing 32% w/w of MCC and 64% w/w of CS, and tablet B containing 10% w/w of CS and 88% w/w of MCC. The comparative study was extended to include a common over-the-counter (OTC) pharmaceutical product (Excedrin tablet). The Sample Planar tool was used to smooth the surface.

In-house prepared tablet A was used for method development and refinement. The team used Clarity software to automatically select peak/baseline points of each component, but recognized that this could be adjusted manually based on library spectra. Consequently, 12 methods were produced based on 12 different peak/baseline selections. Ultimately, the researchers selected method 1 (consisting of the respective peak/baseline wavenumbers: 1,650/1,669 cm^{-1} for midodrine HCl, 1,159/1,187 cm^{-1} for MCC; and 1,142/1,167 cm^{-1} for CS). Results are shown in Figure 6.

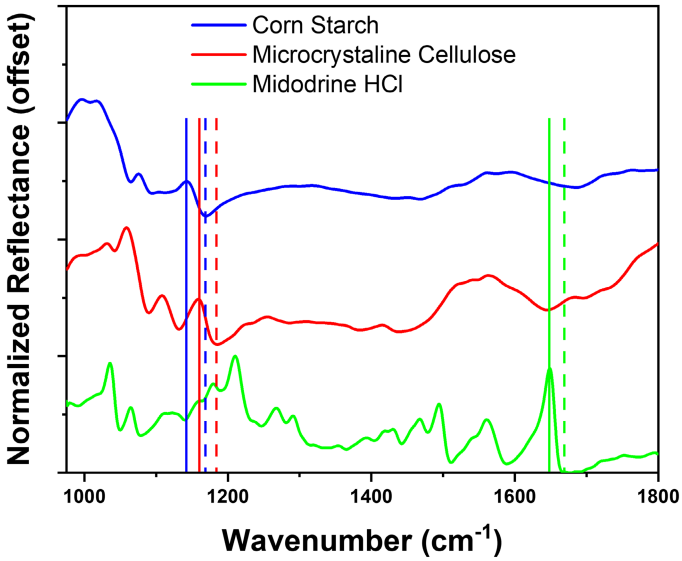

Figure 6. IR reflectance spectra of API, Midodrine HCl ingredients.

Tablet A was also used to investigate the relationship between step (pixel) size and data acquisition time, with sizes of 1, 3, 5, 10, 20, and 40 µm studied (Figure 7). Zaker and team found that step size significantly influenced particle detection and data acquisition time. The authors found that step size significantly influenced particle detection and data acquisition time, and while a pixel size of ≤ 10 µm was optimal for this particular method, they recommended optimizing data acquisition time and step size based on the expected particle size of the components prior to imaging.

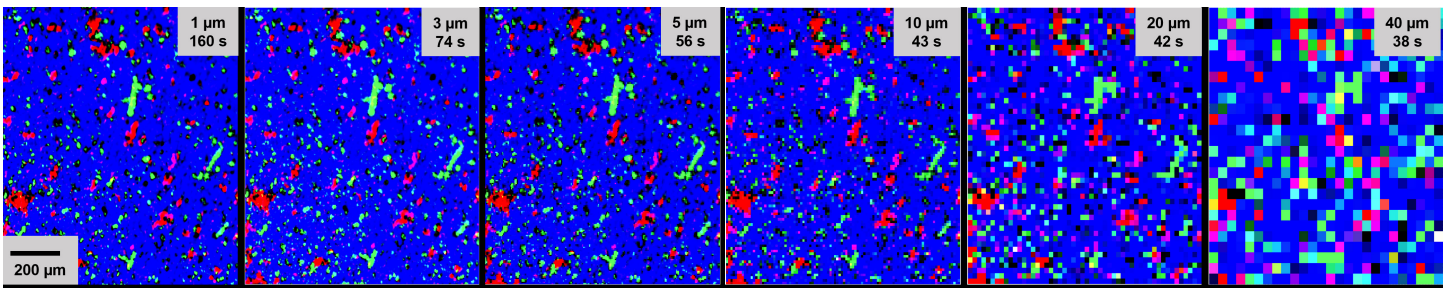

Figure 7. Tablet A. Effect of pixel size (1 to 40 µm resolution).

The in-house prepared tablets A and B were used to compare LDIR and Raman imaging (Figure 8). Zaker and team reported the 8700 LDIR imaging demonstrated "good agreement with Raman but reduce[d] acquisition times ~ 100x." The authors stated, "LDIR imaging detects APIs and excipients in pharmaceutical formulations effectively," with "API percent area coverage comparable for the analyzed tablets between techniques." Notably, the authors observed that the 8700 LDIR detected a greater number of particles compared to Raman imaging, with a consistently smaller mean Feret diameter in the LDIR images, as similarly observed in the previous paper by Carruthers *et al.*

The authors also assessed an OTC Excedrin tablet using a step size of 20 µm, citing that preliminary Raman mapping at a 10 µm step size required an extendedly long acquisition time of approximately two weeks. A comparative analysis demonstrated no significant differences in surface morphologies between LDIR and Raman images; however, the 8700 LDIR was able to detect a greater number of domains for APIs with a smaller Feret diameter again observed.

Key quotes from the study:

"Overall, LDIR imaging was evaluated as a potential rapid, at-line tool for characterization of size and distribution of components within pharmaceutical tablets. Improving data acquisition times while maintaining specificity and resolution compared with other chemical imaging techniques, LDIR imaging could prove valuable for enhancing drug product manufacturing and process understanding."

"LDIR reflectance imaging offers a promising alternative for rapid analysis of pharmaceuticals without scarifying the desired physicochemical information."

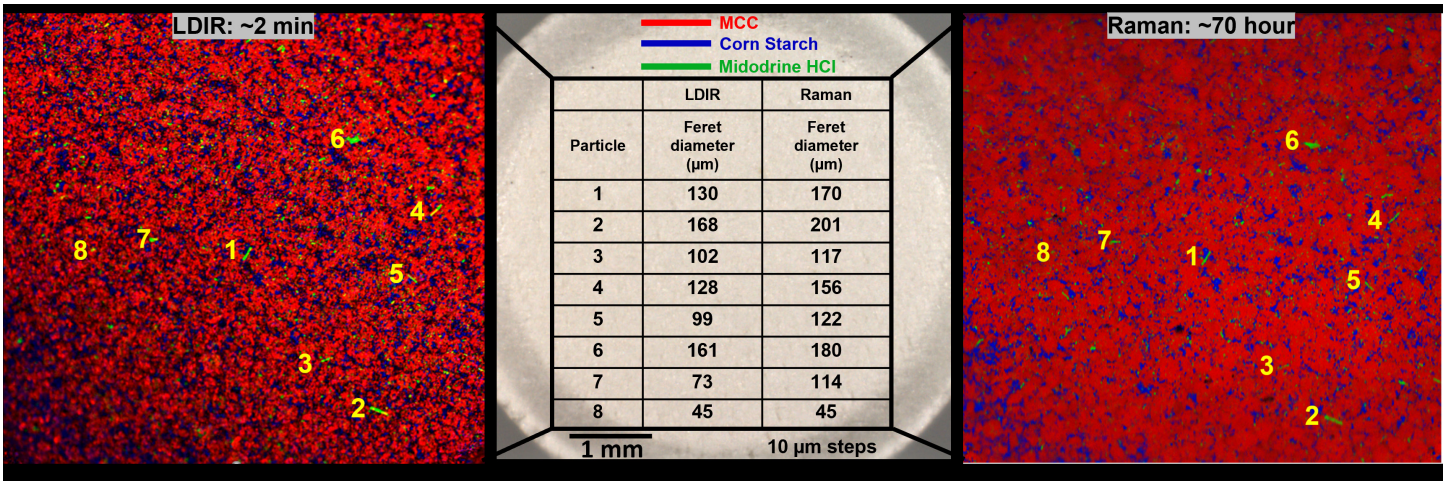

Particle	LDIR Feret diameter (µm)	Raman Feret diameter (µm)
1	130	170
2	168	201
3	102	117
4	128	156
5	99	122
6	161	180
7	73	114
8	45	45

Figure 8. Comparative LDIR and Raman images of in-house tablet B, with domains analyzed marked. Reprinted from Zaker *et al.*, "Assessment of Laser Directed Infrared (LDIR) Imaging for a Physicochemical Approach to In Vitro Characterization of Pharmaceutical Tablets" 2023 FDA Science Forum. Copyright © 2023 U.S. FDA/CDER.

Tissue analysis

Biodegradable Multi-Layered Silk Fibroin-PCL Stent for the Management of Cervical Atresia: In Vitro Cytocompatibility and Extracellular Matrix Remodeling In Vivo[10]

Ojha and collective researchers, from the Indian Institute of Technology Kharagpur and the Institute of Reproductive Medicine, Kolkata, India, developed a multilayered biodegradable cervical stent to address cervical atresia (CA). CA is a rare congenital Mullerian duct anomaly where the cervix is absent or deformed and nonfunctional, producing a physical blockage or obstruction in the cervix. This obstruction can cause chronic pelvic pain, menstrual absence despite normal hormonal cycles, and long-term complications that can damage the uterus and affect fertility. Treatment involves nonconservative surgical procedures like hysterectomy (complete removal of the uterus and cervix to avoid severe issues like hematometra and retrograde menstruation), and conservative procedures like cervical reconstruction or laparoscopic-assisted surgery to conserve the reproductive organs for future fertility. These procedures remain challenging for clinicians. Ojha *et al.* noted the increasing progress of cervical reconstruction using tissue engineering approaches; silk fibroin (SF) protein from *Bombyx mori*; and polycaprolactone (PCL)—a slow-degrading FDA-approved polymer—as extensively researched biomaterials for bioengineering and reproductive health applications.

In this study, Ojha and researchers produced a stent made from a homogeneous blend of SF with PCL using hexafluoroisopropanol as a common solution. The stent (of average length 40 mm and 3 mm diameter) was fabricated using electrospinning for fibrous outer/inner sheets, and 3D printing to create a concentric cylinder of honeycomb middle layer. The authors used an in vivo model (Wistar rat) for stent studies, and in vitro cytocompatibility studies (human cervical squamous cells, columnar epithelial cells, and endometrial stromal cells).

The in vivo stent study was conducted for 10 days, 30 days, and 60 days (n = 3 for each time interval) and then explanted (S10, S30, and S60) at definite time intervals and fixed in neutral buffered formalin. The 8700 LDIR was used to analyze the localization of extracellular matrix (ECM) proteins—particularly collagen I (COL I)—as well as stent components and tissue integration within the explants. The explants were mounted over low-e microscope slides. Using Clarity software, 10 spectra were taken of each explant and used to make a reference spectrum. A single peak ratio analysis was made for each pretargeted constituent using the reference spectra.

molecule name	peak wavenumber (cm^{-1})	assignment
PCL	1163, 1458,1734	CH_2 deformation, CH_3 bending [*Strong*]
SF	1065,1365, 1628	amide region I, II medium
COL I	1306,1336	[*Strong*]

Figure 9. LDIR peak/baseline wavenumbers for targeted constituents, PCL, SF, and COL I.

As per Ojha *et al.*, "LDIR imaging provide[d] tissue molecular and structural insights in situ without sample processing or labeling." LDIR imaging of the explants indicated: deposition and localization of COL I; ECM proteins at the outer layer; that the SF/PCL were the main components of the stent; and that there was uniform distribution across explants. The localization studies were useful in proving continued patency post-implantation in the animal models.

Key quote from the study:

"LDIR imaging provides tissue molecular and structural insights in situ without sample processing or labeling."

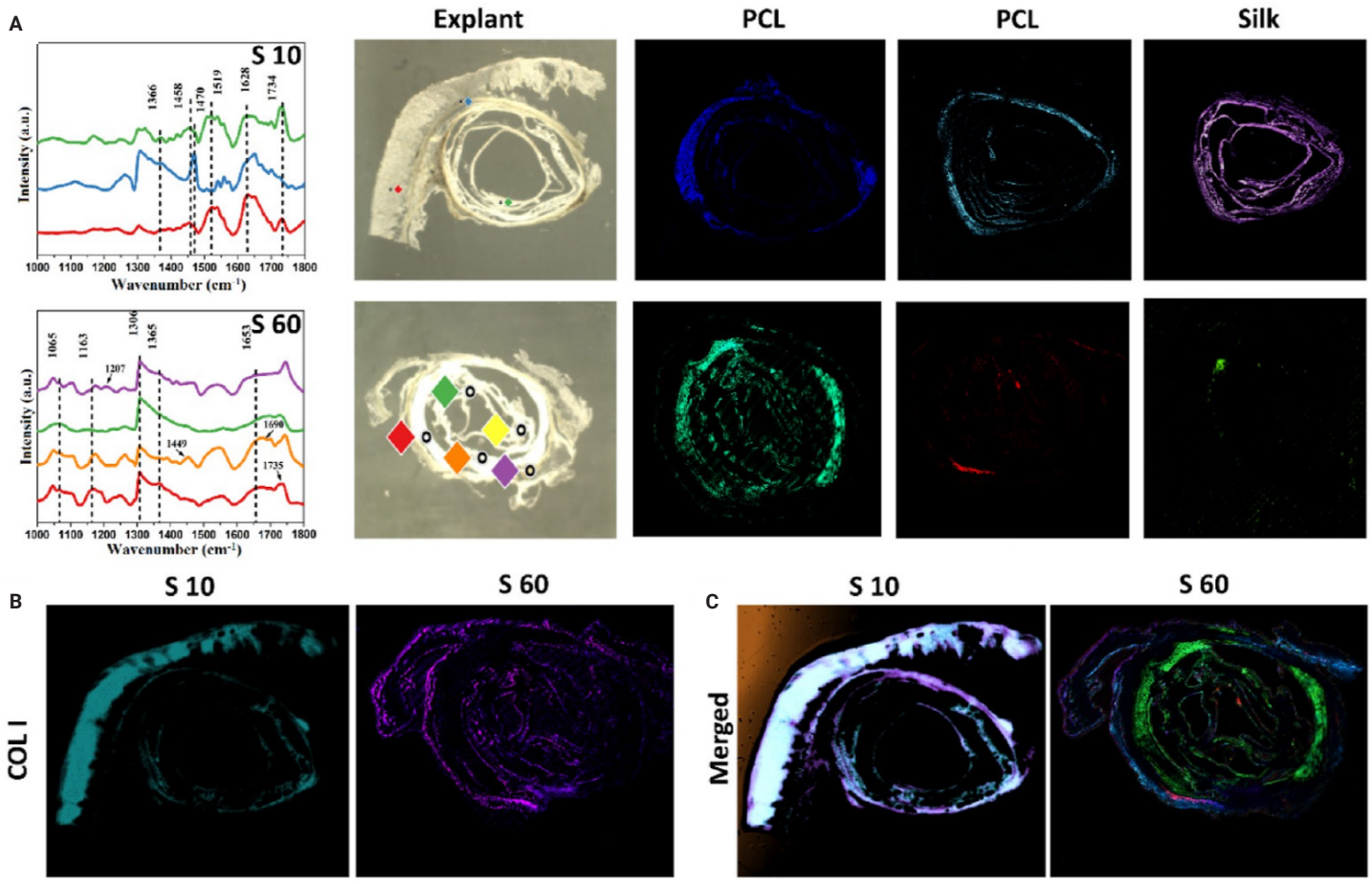

Figure 10. LDIR spectra and imaging of explants showing the (A) FTIR spectra and spatial distribution of SF and PCL in explants at time intervals, S10 and S60; (B) COL I mapping across the explants; and (C) merged LDIR images. Reprinted with permission from Ojha *et al.*, *ACS Appl. Mater. Interfaces* **2023**, *15, 33*, 39099–39116. Copyright © 2023 American Chemical Society.

Food and beverage

Rapid Analysis of Food Raw Materials Adulteration Using LDIR Spectroscopy and Imaging[11]

Da Costa Filho, Cobuccio, and team, from Switzerland-based Nestlé Research investigated the suitability of the 8700 LDIR as a rapid, untargeted screening technology for detection, identification and semiquantification of adulterants in food ingredients.

The authors noted that plant-based protein and nitrogen-rich compounds are commonly used as cost-effective (economic) adulterants to increase the apparent protein concentration in various dehydrated commodities. They also identified that current analytical methods developed for the detection of nitrogenous compounds in food are either quick but limited to few compounds or few food matrices, or cover several matrices up to low limits of detection. Vibrational spectroscopy had previously and commonly been used in testing food authenticity and adulteration for many years, but it can be a time-intensive and computationally intensive technique. Therefore, the authors were interested in investigating LDIR imaging as a quick and intuitive screening tool, with extended application of mid-IR on dehydrated food matrices.

The team investigated two fraudulent processes: dry blending and wet blending. Five raw food matrices were adulterated with a combination of nitrogen-rich compounds, foreign protein, and bulking agents. Commercial samples of skimmed milk powder (SMP; n = 45), soy protein isolate (SPI; n = 31), chicken meat powder (CMP; n = 35), pea protein isolate (PPI; n = 32), and wheat flour (WF; n = 6) were dry-blended adulterated at varying concentrations between 1 and 15% (w/w), and a further ten samples of SMP were wet-blended adulterated at 5 and 10% (w/w). Powder samples were pressed into pellets of 13 mm diameter and 2 to 3 mm thickness. The researchers affixed the pellets to the microscope slide using optical adhesive, with the top

layer microtomed by the Sample Planar tool to create a flat surface—the process taking "about 5 minutes."

The team created IR chemical imaging methods in Clarity software to screen for adulterants and to classify ingredient distribution for surface area concentration. First, the researchers created a custom spectral library of pure ingredients, collecting spectra in both direct reflectance and ATR modes at 0.5 cm^{-1} data point spacing and at 8 cm^{-1} spectral resolution. They then selected the most relevant wavenumbers for screening adulterants, based on spectral features related to the raw food matrices and the adulterants. One peak combination-based (uses four wavenumbers) and three peak ratio-based (uses two wavenumbers, at peak/baseline positions) screening methods were created, enabling the instrument to quickly scan the sample area, acquire an IR image contrast to inspect contamination, and get an answer in the form of "yes" or "no." The authors cited that the peak ratio accounted for topography differences on the sample surface, and provided contrast solely due to chemical differences on the sample. The authors also utilized the Clarity software algorithm for creation of the method for classification of ingredients. Taking "less than a minute," Clarity software automatically selected peak/baseline wavenumbers that best distinguished the ingredients, with no need for chemometrics or calibration standards.

IR chemical images were acquired on the pellet surfaces, taking "about 6 minutes to scan the area of 13 mm diameter... with all four screening methods at 20 µm pixel size" to detect abnormal samples. Chemical classification images were acquired in "about 1 to 7 minutes, depending on the number of ingredients present in the sample," using 20 µm pixel resolution. The identification of food adulterants was performed in 25 minutes.

The researchers observed characteristic fingerprint profiles in the mid-IR spectra, allowing identification of the raw ingredients, nitrogen-rich compounds, or bulking agents. The authors also discussed challenges in detecting and identifying animal/plant-based protein from foreign sources rich in protein, especially when added to food matrices of similar proteins (such as skimmed milk powder, plant flours, and meat powders). This is because the spectra of intact and hydrolyzed proteins would show similar intensity and shape of absorption bands. Similarly, when adulterants are homogeneously dispersed or hidden within the particles, they can also be difficult to detect with mid-IR technology. The researchers observed difficulty in detecting nitrogen-rich compounds in wet-blended samples, likely related to the solubility of the adulterants allowing homogeneous dispersion.

For dry-blended adulteration, the authors observed sensitivity of 82% for samples adulterated at 1% and sensitivity from 92 to 100% for samples adulterated at ≥ 5% economic adulteration. Notably, the authors highlighted the sensitivity of the LDIR technology in "detecting very low levels of food adulterants (e.g. guanidine at 0.06%)."

Key quotes from the study:

"LDIR showed promising results for screening analysis of economically motivated adulteration (> 5%) in food matrices."

"The results reported in this study shows great potential of LDIR technique to use for food adulteration detection."

Conclusion

Leading research groups around the world have demonstrated the utility of the Agilent 8700 LDIR chemical imaging system with Agilent Clarity software across diverse applications, such as pharmaceutical formulations, food authenticity testing, adhesive surface chemistry, and biomaterials. These studies highlight the versatility of the 8700 LDIR with Clarity software as a next-generation IR imaging platform. By enabling rapid, automated, and spatially resolved chemical analysis, the 8700 LDIR system expands the possibilities for users to tackle challenges in quality control, authenticity verification, material design, and biomedical innovation.

Additional information

- Agilent 8700 LDIR chemical imaging system
- Agilent Clarity software
- 8700 LDIR system specifications
- Best practices
- Spectroscopy supplies
- Microplastics technologies FAQs

References

1. Gowen, A. A.; O'Donnell, C. P.; Cullen, P. J.; Bell, S. E. J. Recent Applications of Chemical Imaging to Pharmaceutical Process Monitoring and Quality Control. European *Journal of Pharmaceutics and Biopharmaceutics* **2008**, *69(1)*, 10–22. https://doi.org/10.1016/j.ejpb.2007.10.013.
2. Alvarez-Fernandez, A.; Pawar, N.; Sanchez-Puga, P.; Zaccai, Nathan. R.; Maestro, A. Peptide-Guided Self-Assembly: Fabrication of Tailored Spiral-like Nanostructures for Precise Inorganic Templating. *Advanced Functional Materials* **2024**, *35(1)*, 2411061. https://doi.org/10.1002/adfm.202411061.
3. Gordon, N.; Beaudoin, H.; Kelso, P. R.; Southwell, B.; Wright, D. D. Laser Direct Infrared Spectroscopy Hyperspectral Imaging; Applications in Geochemical Phase Mapping and Interpretation of Multidimensional Analysis. [online] American Geophysical Union 2024. 2024. Available at: https://www.researchgate.net/publication/386508728_Laser_Direct_Infrared_Spectroscopy_Hyperspectral_Imaging_Applications_in_Geochemical_Phase_Mapping_and_Interpretation_of_Multidimensional_Analysis [Accessed Feb. 2026].
4. Gordon, N.; Beaudoin, H.; Kelso, P. R.; Southwell, B.; Wright, D. D. Laser Direct Infrared Spectroscopy Hyperspectral Imaging; Applications in Geochemical Phase Mapping and Interpretation of Multidimensional Analysis. [online] ESS Open Archive December 27, 2024, https://doi.org/10.22541/essoar.173532426.64038391/v1 [Accessed Feb. 2026].
5. Zhou, X.; Zheng, H.; Wu, Y.; Yin, H.; Mao, X.; Li, N.; Guo, H.; Chang, Y.; Jiang, X.; Ai, Q.; Xue, C. Scalable Production of Muscle and Adipose Cell-Laden Microtissues Using Edible Macroporous Microcarriers for 3D Printing of Cultured Fish Fillets. *Nature Communications* **2025**, *16*, 1740. https://doi.org/10.1038/s41467-025-57015–1.
6. Sacré, P.-Y.; Alaoui Mansouri, M.; De Bleye, C.; Coïc, L.; Hubert, Ph.; Ziemons, E. Evaluation of Distributional Homogeneity of Pharmaceutical Formulation Using Laser Direct Infrared Imaging. I*nternational Journal of Pharmaceutics* **2022**, *612*, 121373. https://doi.org/10.1016/j.ijpharm.2021.121373.
7. Carruthers, H.; Clark, D.; Clarke, F. C.; Faulds, K.; Graham, D. Evaluation of Laser Direct Infrared Imaging for Rapid Analysis of Pharmaceutical Tablets. *Analytical Methods* **2022**, *14(19)*, 1862–1871. https://doi.org/10.1039/d2ay00471b.
8. Zaker, Y.; Yilmaz, H.; Lex, T. R.; Guo, C.; Rodriguez, J. D.; Willett, D. R. Advancing Pharmaceutical Tablet Analysis with Laser Direct Infrared (LDIR) Imaging. *Journal of Pharmaceutical and Biomedical Analysis* **2025**, *262*, 116897. https://doi.org/10.1016/j.jpba.2025.116897.
9. Zaker, Y., Yilmaz, H.; Willett, D. (2023). *Assessment of Laser Directed Infrared (LDIR) Imaging for a Physicochemical Approach to In Vitro Characterization of Pharmaceutical Tablets*. [online] 2023 FDA Science Forum. 2023. Available at: https://www.fda.gov/science-research/fda-science-forum/assessment-laser-directed-infrared-ldir-imaging-physicochemical-approach-in-vitro-characterization [Accessed Feb. 2026].
10. Ojha, A. K.; Rajasekaran, R.; Hansda, A. K.; Singh, A.; Dutta, A.; Seesala, V. S.; Das, S.; Dogra, N.; Sharma, S.; Goswami, R.; *et al.* Biodegradable Multi-Layered Silk Fibroin-PCL Stent for the Management of Cervical Atresia: In Vitro Cytocompatibility and Extracellular Matrix Remodeling in Vivo. *American Chemical Society Applied Materials & Interfaces* **2023**, *15(33)*, 39099–39116. https://doi.org/10.1021/acsami.3c06585.
11. da Costa Filho, P. A.; Cobuccio, L.; Mainali, D.; Rault, M.; Cavin, C. Rapid Analysis of Food Raw Materials Adulteration Using Laser Direct Infrared Spectroscopy and Imaging. *Food Control* **2020**, *113*, 107114. https://doi.org/10.1016/j.foodcont.2020.107114.
12. Yeh, K.; Kenkel, S.; Liu, J.-N.; Bhargava, R. Fast Infrared Chemical Imaging with a Quantum Cascade Laser. *Analytical Chemistry* **2014**, *87(1)*, 485–493. https://doi.org/10.1021/ac5027513.
13. Hildebrandt, L.; Zimmermann, T.; Sobakpo, M.; Hahn, K.; Pröfrock, D. A Validated, Cost-Effective Alternative: Gold-Coated vs. Aluminum-Coated Membranes for LDIR Microplastic Analysis. **2025**.

14. Huang, X.; Li, C.; Jiang, S.; Wang, X.; Zhang, B.; Liu, M. Supramolecular Chirality of the Hydrogen-Bonded Complex Langmuir–Blodgett Film of Achiral Barbituric Acid and Melamine. *Journal of Colloid and Interface Science* **2005**, *285(2)*, 680–685. https://doi.org/10.1016/j.jcis.2004.12.025.
15. Huang, X.; Li, C.; Jiang, S.; Wang, X.; Zhang, B.; Liu, M. Self-Assembled Spiral Nanoarchitecture and Supramolecular Chirality in Langmuir–Blodgett Films of an Achiral Amphiphilic Barbituric Acid. *Journal of the American Chemical Society* **2004**, *126(5)*, 1322–1323. https://doi.org/10.1021/ja036878i.
16. Zhang, Y.; Chen, P.; Jiang, L.; Hu, W.; Liu, M. Controllable Fabrication of Supramolecular Nanocoils and Nanoribbons and Their Morphology-Dependent Photoswitching. *Journal of the American Chemical Society* **2009**, *131(8)*, 2756–2757. https://doi.org/10.1021/ja805891k.
17. Wen, H.; Yao, J.; Chen, X.; Ling, S.; Shao, Z. Silk-Derived Peptide Nanospirals Assembled by Self-Propelled Worm-like Filaments. *Nano Research* **2022**, *16(1)*, 1414–1420. https://link.springer.com/article/10.1007/s12274-022-4671-1.

www.agilent.com

RA260427.708

Printed in the USA, May 18, 2026
5994-9040EN

Agilent
Trusted Answers